THE JOURNAL OF BIOLOGICAL CHEMISTRY VOL. 285, NO. 24, pp. 18485–18495, June 11, 2010

The Silencing Mediator of Retinoid and Thyroid Hormone Receptors (SMRT) Regulates Adipose Tissue Accumulation and Adipocyte Insulin Sensitivity *in Vivo*[*]

Received for publication, January 25, 2010, and in revised form, April 1, 2010 Published, JBC Papers in Press, April 6, 2010, DOI 10.1074/jbc.M110.107680

Maria M. Sutanto[‡], Kelly K. Ferguson[§], Hiroya Sakuma[§], Honggang Ye[§], Matthew J. Brady[‡§], and Ronald N. Cohen[‡§1]

From the [‡]Committee on Molecular Metabolism and Nutrition, Division of the Biological Sciences and the [§]Section of Endocrinology, Diabetes, and Metabolism, Department of Medicine, The University of Chicago, Chicago, Illinois 60637

The silencing mediator of retinoid and thyroid hormone receptors (SMRT) serves as a corepressor for nuclear receptors and other factors. Recent evidence suggests that SMRT is an important regulator of metabolism, but its role in adipocyte function *in vivo* remains unclear. We generated heterozygous SMRT knock-out ($SMRT^{+/-}$) mice to investigate the function of SMRT in the adipocyte and the regulation of adipocyte insulin sensitivity. We show that $SMRT^{+/-}$ mice are normal weight on a regular diet, but develop increased adiposity on a high-fat diet (HFD). The mechanisms underlying this phenotype are complex, but appear to be due to a combination of an increased number of smaller subcutaneous adipocytes as well as decreased leptin expression, resulting in greater caloric intake. In addition, adipogenesis of mouse embryonic fibroblasts (MEFs) derived from these mice was increased. However, adipocyte insulin sensitivity, measured by insulin-induced Akt phosphorylation and insulin-mediated suppression of lipolysis, was enhanced in $SMRT^{+/-}$ adipocytes. These finding suggest that SMRT regulates leptin expression and limits the ability of fat mass to expand with increased caloric intake, but that SMRT also negatively regulates adipocyte insulin sensitivity.

The adipocyte plays an active and indispensable role in energy homeostasis, and obesity is associated with numerous metabolic and other pathologies (1, 2). Classically viewed as an inert energy storage depot involved in lipid metabolism, recent studies have shown that the adipocyte is an active endocrine organ that secretes a number of factors collectively termed adipokines. One such factor, leptin, was identified as the gene product found to be lacking in *ob/ob* mice, and these mice exhibit profound obesity and hyperphagia (3). Leptin has since been shown to exert its effects centrally at the hypothalamus to regulate feeding behavior (4, 5, 6) and peripherally to promote energy expenditure (7, 8, 9). Circulating leptin levels generally correlate with whole body adiposity (10, 11) and are subject to regulation by feeding and fasting (12, 13).

Adipocyte differentiation, or adipogenesis, is regulated by a variety of factors, and the central regulator of adipogenesis is considered to be the peroxisome proliferator-activated receptor γ (PPARγ)[2] (14). PPARγ is a member of the nuclear hormone receptor (NR) family and is enriched in adipose tissue, where it also serves to maintain the mature adipocyte phenotype (15). Although its endogenous ligand has not been identified, PPARγ has been shown to be the molecular target for the thiazolidinedione (TZD) class of drugs used to treat type 2 diabetes (16). Although TZDs improve insulin sensitivity, glucose tolerance, and lipid homeostasis, these beneficial metabolic effects are often accompanied by increased adipose mass (17, 18) and other side effects. A potential mechanism of TZD action is the partitioning of free fatty acids (FFAs) from extra-adipose organs to the adipose tissue for appropriate storage. Distinct white adipose tissue (WAT) depots seem to possess varying responsiveness to TZD treatment, with subcutaneous WAT responding more robustly as compared with visceral WAT (19, 20).

Transcriptional control by NRs, including PPARγ and others, depends on multiprotein coregulatory complexes. In general, corepressor complexes are recruited to NRs in the absence of ligand or the presence of antagonists, whereas coactivator complexes are recruited to NRs in the presence of agonists (21). Coactivators and corepressors modulate gene transcription by a variety of mechanisms, include histone acetylation, chromatin remodeling, and direct interactions with basal transcription complexes. Although certain such coregulators have been implicated in the regulation of energy homeostasis (22), the underlying mechanisms of corepressor function in metabolic tissues remains unclear.

The two major NR corepressors are the silencing mediator of retinoid and thyroid hormone receptors (SMRT) and the nuclear receptor corepressor (NCoR) (23, 24, 25). We have previously shown that down-regulation of SMRT and NCoR expression in 3T3-L1 cells leads to enhanced adipocyte differentiation, in part through increased PPARγ transcriptional activity (26). Whereas SMRT has been shown to play a role in regulating immune response (27), mediating DNA repair (28), and in neuronal differentiation and cardiac development (29, 30), its role in adipogenesis, adipocyte function, and energy

* This work was supported, in whole or in part, by National Institutes of Health Grant NIDDK R01 DK078125 and an Endocrine Society Bridge Grant.

[1] To whom correspondence should be addressed: Section of Endocrinology, Diabetes, and Metabolism, Dept. of Medicine, The University of Chicago, 5841 S. Maryland Ave., MC 1027, Chicago, IL 60637. Tel.: 773-702-5770; Fax: 773-834-0486; E-mail: roncohen@medicine.bsd.uchicago.edu.

[2] The abbreviations used are: PPARγ, peroxisome proliferator-activated receptor γ; BAT, brown adipose tissue; FFA, free fatty acid; HFD, high-fat diet; MEF, mouse embryonic fibroblast; NCoR, nuclear corepressor; NR, nuclear hormone receptor; qRT-PCR, quantitative reverse transcriptase-polymerase chain reaction; SMRT, silencing mediator of retinoid and thyroid hormone receptors; TZD, thiazolidinedione; WAT, white adipose tissue; WT, wild-type; GTT, glucose tolerance test; ITT, insulin tolerance test.

homeostasis *in vivo* remains uncertain. Nofsinger *et al.*, (31) studied a mutant SMRT knock-in with deficient interactions with nuclear receptors ($SMRT^{mRID}$ mice) to show that SMRT regulates PPARγ and thyroid hormone receptor (TR) signaling *in vivo*. $SMRT^{mRID}$ mice exhibited reduced respiration, glucose intolerance, and impaired muscle insulin sensitivity (on a regular diet), and increased adiposity. Although adipocyte insulin sensitivity was felt to be normal based on normal fasting and insulin-suppressed free fatty acid levels, a focused evaluation of adipocyte function was not performed. In addition, although there were increased adipose tissue stores, the total body size of $SMRT^{mRID}$ mice was reduced. In the present study, we generated SMRT knock-out mice to investigate the role of SMRT in adipogenesis and adipocyte function, particularly in response to high-fat feeding. We found that although $SMRT^{+/-}$ mice exhibited normal weight on a regular diet, these mice developed increased weight and adiposity when challenged with a high-fat diet (HFD), because of a combination of an increased number of smaller subcutaneous adipocytes and increased caloric intake. The latter appears to be dependent on abnormal regulation of leptin gene expression in $SMRT^{+/-}$ adipocytes. Surprisingly, however, when mice were fed a HFD, adipocytes isolated from these mice exhibited enhanced insulin signaling when compared with adipocytes derived from wild-type (WT) mice, suggesting that SMRT directly regulates adipocyte insulin sensitivity in addition to the ability of adipose stores to expand in response to HFD.

EXPERIMENTAL PROCEDURES

Transgenic Mouse Generation—An embryonic stem (ES) cell line containing a gene trap within the *SMRT* gene was obtained from the Mutant Mouse Regional Resource Center (MMRRC) at University of California, Davis. The gene trap insertion codes for the β-galactosidase gene with an in-frame stop codon. We identified the integration site of the targeting cassette between exons 9 and 10 of full-length SMRT; these exons are present in all known SMRT transcripts and are proximal to exons coding for nuclear receptor-interacting domains. ES cells containing the gene trap insertion was microinjected into the pronuclei of 129 mice. Potential founders were screened by utilizing PCR primers homologous to the gene trap (forward: CAAATGGCGATTACCGTTGA; reverse: TGCCCAGTCATAGCCGAATA); amplification for the T cell receptor δ gene was used as a PCR control (forward: CAAATGTTGCTTGTCTGGTG; reverse: GTCAGTCGAGTGCACAGTTT) (Fig. 1*B*). Multiple founders were identified and two $SMRT^{+/-}$ males were selected for propagation of independent lines for characterization. Both lines were backcrossed to the C57BL/6 background for at least 6 generations. DNA samples isolated from tail clips of subsequent litters were screened by PCR as described above.

Mouse Treatment and Care—Mice were housed in a specific pathogen-free barrier facility with a 12-h light/dark cycle, with free access to water and a standard chow diet at the University of Chicago. We used age-matched male littermates for each experiment. All animal husbandry and animal experiments were approved by the University of Chicago Institutional Animal Care and Use Committee. After weaning at 3 weeks of age, tail clippings were obtained for genotyping by PCR, and mice were weighed weekly. At 3 months of age, male mice were sacrificed by CO_2 narcosis for the studies described throughout. Brain, spleen, skeletal muscle, liver, pancreas, BAT, and epididymal, perirenal, and subcutaneous WAT were harvested, frozen on dry ice and stored at −80 °C for subsequent studies. Blood was collected by cardiac puncture, stored at 4 °C overnight and centrifuged at 3,500 rpm, 4 °C for 15 min to obtain serum.

For the HFD studies, 2-month-old male $SMRT^{+/-}$ and $SMRT^{+/+}$ mice were fed HFD (45% of calories from fat; D12451, Research Diets, Inc.) for 4 weeks. Mice were weighed twice weekly over the course of the 4 weeks.

Indirect Calorimetry—3-month-old male $SMRT^{+/-}$ and $SMRT^{+/+}$ mice were individually placed in the respiratory chambers of LabMaster System (TSE Systems, Inc, Chesterfield, MO). Mice were acclimated to the chambers for 2–3 days before O_2 consumption, CO_2 production, energy expenditure, locomotor movement, and food and water consumption (per mouse) were recorded for the following 3 days.

Mouse Embryonic Fibroblast (MEF) Adipogenesis Studies—For preparation of primary MEFs, embryonic day 13.5 embryos were minced and digested with TrypLE Express (Invitrogen). Cells were collected and cultured at 37 °C in Dulbecco's modified Eagle's medium (Invitrogen) supplemented with 10% fetal bovine serum (Aleken Biologicals, Nash, TX). Cells after one passage were plated to 35-mm tissue culture dishes and propagated to confluence. We induced confluent MEFs to undergo adipogenesis by incubating them first for 4 days with a differentiation induction medium modified from Wabitsch *et al.* (32), and containing 10% fetal bovine serum, 10 μg/ml human transferrin (Sigma), 1 μg/ml insulin (Millipore), 100 nM cortisol (Sigma), 0.2 μM T3 (Sigma), 0.25 μM dexamethasone (Millipore), 0.5 mM MIX (Sigma), and 10 μM Troglitazone; and then for an additional 4 days with a medium containing only the human transferrin, insulin, cortisol, and T3, with refreshment of medium every 2 days. At days 0, 4, and 8 postinduction, cells were used for protein analyses as described below. At day 8 postinduction, the appearance of cytoplasmic lipid accumulation was stained with Oil Red O. Embryo heads and limbs were excised and used for genotyping. Briefly, the non-fibroblast tissues were minced in lysis buffer for genomic DNA isolation. Genotyping of MEFs was conducted by PCR as described above. Zygosity was determined by utilizing PCR primers homologous to the wild-type SMRT locus immediately upstream and downstream of the gene trap (forward: GAGAGAGGGTCTCCATGCTGCAG; reverse: GCTGCAGTCTGTCCCATCTACTG) and a PCR primer homologous to the gene trap (reverse: CAGGCTGCGCAACTGTTGGG). Amplification for the WT and mutant alleles yielded PCR amplicons of 405 bp and 1552 bp in length, respectively.

Metabolic Studies—Glucose and insulin tolerance tests (GTT, ITT) were performed on 3-month-old male mice that were fasted overnight and for 6 h, respectively. For GTT, animals were injected 2 g/kg D-glucose ip; whereas for ITT, 0.75 units/kg human insulin (90356, Millipore, Billerica, MA) was injected intraperitoneal glucose levels were measured from tail bleeds at 0, 15, 30, 45, 60, 90, and 120 min after ip injection using an Ascensia Contour blood glucose meter (Bayer). For GTT,

blood was collected by tail bleed at 0 and 30 min after ip glucose injection for measurement of serum insulin levels as described below.

RNA Analyses—Total RNA from WAT was extracted using RNeasy Plus Mini Kit according to manufacturer's directions (Qiagen, Valencia, CA) before cDNA synthesis was performed by using the iScript cDNA synthesis kit (Bio-Rad). Experiments were performed as described in the manual for ABI Prism 7900 HT Taqman (AB Applied Biosystems, Foster City, CA) with minor modifications. Each cDNA sample in triplicate was subjected to three individual PCR analysis using the leptin, GAPDH, or PPIA primer pair. For real-time analysis, every PCR reaction was amplified in ABsolute QPCR ROX Mix (Thermo Fisher Scientific, Waltham, MA).

Protein Analyses—Immunoblotting was performed as previously described (33). Briefly, tissues were lysed with a glass Dounce homogenizer in radioimmune precipitation assay buffer (1× PBS, 0.1% SDS, 0.5% sodium deoxycholate, 1% Igepal CA-630, and protease inhibitors). Similarly, cultured primary mouse embryonic fibroblasts were washed with 1× phosphate-buffered saline before lysis with radioimmune precipitation assay buffer. Protein samples were sonicated at an amplitude of 40 with an ultrasonic processor (Sonics & Materials, Inc., Newtown, CT) with five 1-s pulses before they were nutated at 4 °C for 30 min. Next, samples were centrifuged at 4 °C at 13,200 rpm for 30 min. Protein concentrations were determined by the bicinchoninic acid (BCA) protein assay (23227, Thermo Scientific, Waltham, MA) for normalization of protein loading. Insulin signaling experiments were conducted using primary adipocytes isolated from 3-month-old animals as described below. Cells were incubated at 37 °C in supplemented Krebs-Ringer bicarbonate-HEPES (KRBH) buffer with or without 1 nM, 10 nM or 100 nM insulin for 15 min with gentle shaking, placed on ice and then washed three times with KRBH before lysis. Samples were analyzed by SDS-PAGE. Sources of antibodies were the following: anti-SMRT (Abcam); β-actin (Sigma); anti-perilipin (Fitzgerald Industries International, Inc.); anti-cyclophilin A (Millipore); anti-leptin (Bio-Vendor, Candler, NC); anti-PPARγ, anti-C/EBPα; anti-phospho-Akt (Ser-473); and anti-Akt were from Santa Cruz Biotechnology. Immunoblots were developed with the appropriate horseradish peroxidase-conjugated IgG and enhanced chemiluminescence reagents (RPN2132, GE Healthcare Life Sciences).

Primary Adipocyte Isolation—Epididymal and subcutaneous WAT pads were minced in Krebs-Ringer buffer (3.5 ml/g wet weight) supplemented with 25 mM HEPES (pH 7.4), 3% bovine serum albumin, 5 mM glucose, 100 nM (−)-N^6-(2-phenyl-isopropyl) adenosine, and 1 mg/ml type II collagenase (C6885, Sigma). Samples were incubated at 37 °C, with gentle agitation at 80 rpm for 40 min. Isolated primary adipocytes were then transferred to 15-ml conical tubes and centrifuged at 150 rpm for 30 s. Infranatant buffer and stromal-vascular fraction were removed from beneath the adipocyte layer before the primary adipocytes were washed three times with buffer.

Lipolysis Assay—Glycerol and fatty acid (FFA) release from primary adipocytes were monitored as a measure of lipolysis. Primary adipocytes isolated from 3-month-old animals as described above, were used in lipolysis experiments. Freshly isolated primary adipocytes were incubated in KRBH buffer supplemented with 25 mM HEPES (pH 7.4), 3% bovine serum albumin, 5 mM glucose, with or without 10 μM isoproterenol (Sigma) or 1 nM insulin at 37 °C for 1 h with gentle agitation. The infranatant medium was aspirated for measurement of glycerol and free fatty acid content. Glycerol content of the medium was measured using the Free Glycerol Reagent (Sigma). Free fatty acid levels were determined using the NEFA-C assay test kit from Wako (Richmond, VA).

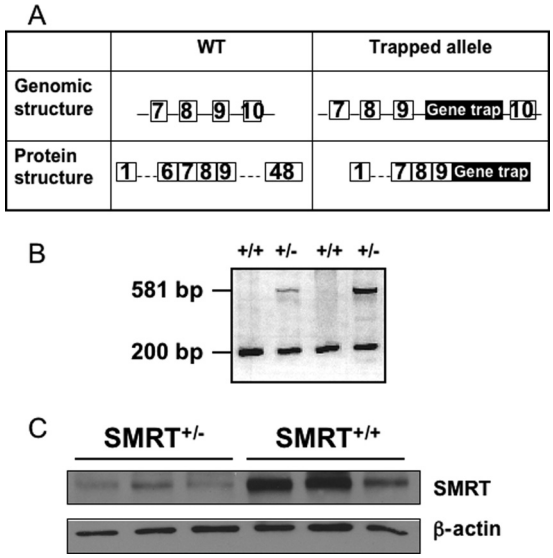

FIGURE 1. **Generation and validation of the SMRT knock-out mouse model.** *A*, transgene design showing introduction of a gene trap cassette that ends with a stop codon in-frame, between exons 9 and 10. *Numbered squares* represent exons in the gene, *solid lines* represent introns, and the *black rectangle* labeled *Gene trap* represents the gene trap insertion. *B*, PCR analysis of genomic DNA from $SMRT^{+/-}$ and WT mice. Primers were designed to amplify both an internal control, T cell receptor δ (200 bp) and the gene trap insertion (581 bp). *C*, SMRT protein levels in epididymal fat pads were determined by Western blotting.

Serum Metabolite Analyses—Serum leptin and insulin levels were measured using the Mouse Leptin ELISA kit and the Ultra Sensitive Mouse Insulin ELISA kit, respectively from Crystal Chem Inc. (Downers Grove, IL). Thyroid function tests were conducted as previously described (34, 35). Briefly, serum TSH was measured using a sensitive, heterologous, disequilibrium, double-antibody precipitation RIA. Serum T_3 and T_4 concentrations were measured by coated tube RIAs (Diagnostic Products, Los Angeles, CA) adapted for mouse serum.

Histology—Isolated WAT were fixed in 10% neutral buffered formalin (pH 7.4) overnight. Fixed WATs were then embedded in paraffin and sectioned by the Immunohistochemistry Core Facility at the University of Chicago. Deparaffined WAT and BAT sections were stained with standard hematoxylin and eosin. Adipocyte area was measured by utilizing ImageJ software (NIH, Bethesda, MD). At least 200 adipocytes per animal were measured.

Freshly isolated livers were frozen in O.C.T. embedding compound (Sakura) in 2-methylbutane and dry ice. Frozen livers were then sectioned and stained with oil red O by the Human Tissue Resource Center at the University of Chicago. Quantity of oil red O staining in livers was quantified using ImageJ software (NIH, Bethesda, MD).

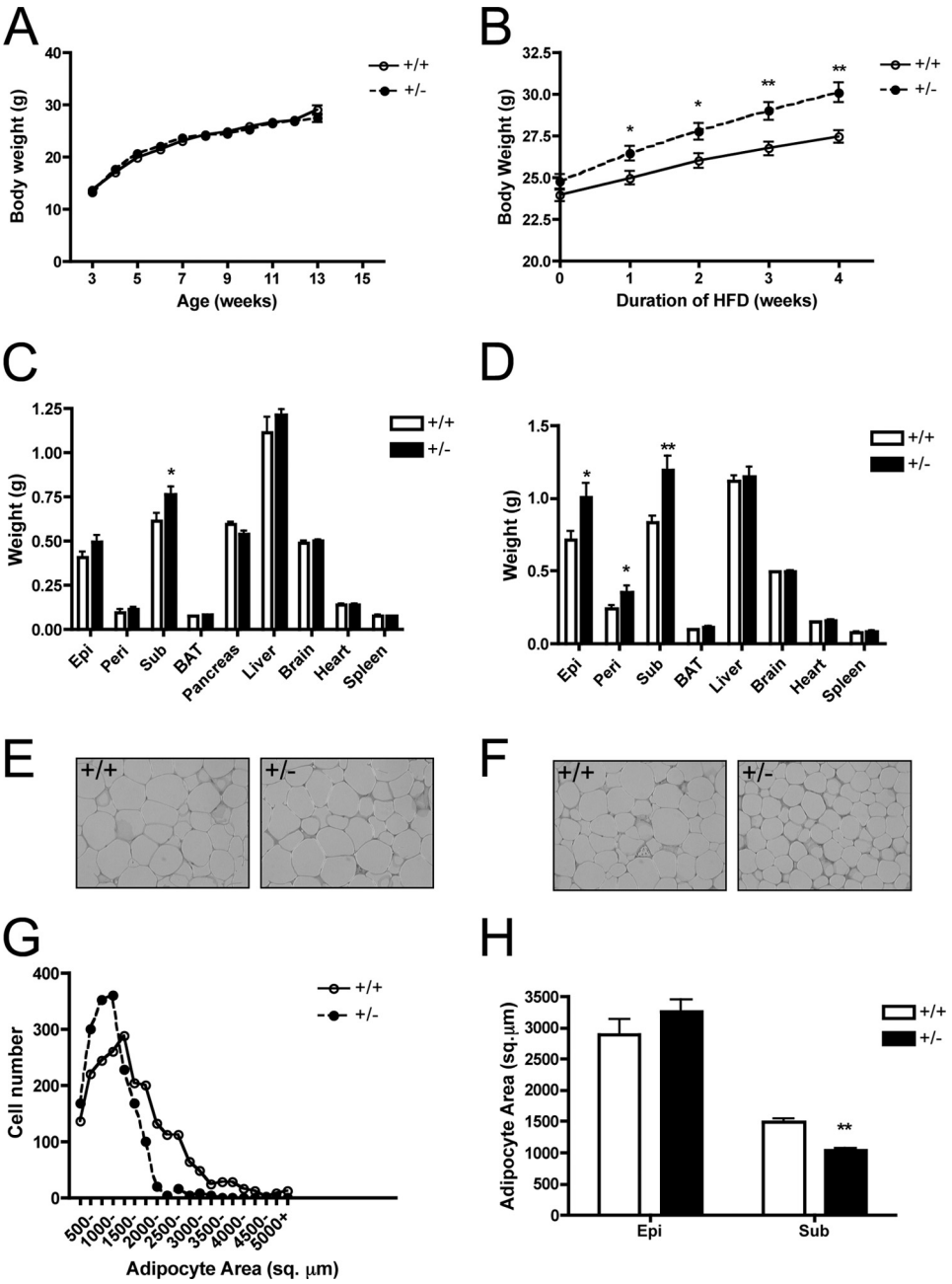

FIGURE 2. **SMRT$^{+/-}$ mice display increased adiposity and are susceptible to diet-induced obesity.** *A*, growth chart of chow-fed mice, $n = 32–40$. *B*, growth chart of mice fed HFD for 4 weeks, $n = 19–21$. *C* and *D*, weight of various tissues from 3-month-old mice fed a chow diet (*C*) or a HFD (*D*), $n = 8–18$. *Epi*, epididymal fat; *Peri*, perirenal fat; *Sub*, subcutaneous fat. *E* and *F*, H&E staining of epididymal (*E*) or subcutaneous (*F*) WAT from 3-month-old HFD-fed SMRT$^{+/-}$ and SMRT$^{+/+}$ mice. *G*, distribution of adipocyte size in subcutaneous WAT from 3-month-old HFD-fed SMRT$^{+/-}$ and WT mice maintained as in *F*, $n = 4$. *H*, analysis of WAT adipocyte size from *G*. *, $p < 0.05$; **, $p < 0.005$ *versus* the corresponding WT value.

Statistical Analyses—The data shown represent means ± S.E. All calculations were performed using Prism 4.0a software (Graphpad Software, Inc., San Diego, CA). Statistical significance between two groups was determined by utilizing unpaired, two-tailed Student's *t* test and considered to be significant at $p \leq 0.05$.

RESULTS

Generation and Validation of SMRT Knock-out Mice—We have previously shown that down-regulation of SMRT expression in 3T3-L1 cells resulted in enhanced adipocyte differentiation, in part through the alteration of PPARγ transcriptional activity (28). To investigate the metabolic consequences of SMRT deletion *in vivo*, we used embryonic stem (ES) cells containing a gene trap between exons 9 and 10 of the SMRT gene locus to generate SMRT knock-out mice (Fig. 1*A*). Two independent lines were randomly chosen for our study. No SMRT$^{-/-}$ offspring survived until birth, most likely due to the intrinsic role of SMRT in neuronal differentiation and cardiac development, as shown previously (29, 30). Thus, we studied heterozygous SMRT knock-out (SMRT$^{+/-}$) mice and their wild-type (WT) littermates in the following experiments. To determine the effects of the gene trap insertion on SMRT protein expression, lysates were prepared from epididymal fat pads for analysis by anti-SMRT immunoblotting. SMRT protein was readily detected in adipocytic lysates from both SMRT$^{+/-}$ and WT mice. As shown in Fig. 1*C*, the expression of SMRT protein was significantly diminished in the SMRT$^{+/-}$ mice, validating our mouse model for the study of the role of SMRT in adipocyte metabolism *in vivo*.

SMRT$^{+/-}$ mice display increased adiposity and susceptibility to diet-induced obesity. Initially, we monitored the body weight of SMRT$^{+/-}$ mice and littermate controls on a regular chow diet. On this diet, there was no significant difference in body weight for WT and SMRT$^{+/-}$ mice (Fig. 2*A*). At 12 weeks of age, we examined individual organs and observed that SMRT$^{+/-}$ mice have significantly larger subcutaneous (SQ) white adipose tissue (WAT) depots than WT mice (Fig. 2*C*), but differences in other fat depots and organ weights were not significantly altered. Next, we subjected 2-month-old mice to a 4-week high-fat diet (HFD) regimen containing 45% of calories derived from fat. Interestingly, SMRT$^{+/-}$ mice gained significantly more weight throughout the course of high-fat feeding (Fig. 2*B*). To determine the cause of the elevated body weight in SMRT$^{+/-}$ mice, we examined individual fat depots and organs. The major white fat pads of SMRT$^{+/-}$ mice were all significantly larger than those of WT mice (Fig. 2*D*). Of note,

$SMRT^{+/-}$ and WT mice displayed no significant differences in the weight of other organs on HFD. Thus, decreasing SMRT expression increases the susceptibility of mice to diet-induced obesity.

$SMRT^{+/-}$ Mice Have More Numerous and Smaller Adipocytes, and SMRT-deficient MEFs Exhibit Increased Adipogenesis—To determine whether the increased adiposity in $SMRT^{+/-}$ mice is due to adipocyte hyperplasia or hypertrophy, we measured the area of individual adipocytes in both epididymal and subcutaneous WAT of $SMRT^{+/-}$ and WT mice (Fig. 2, *E* and *F*). The adipocytes from both groups on chow diet were similar in size. On HFD, epididymal WAT adipocytes from both groups were also of comparable size (Fig. 2*H*). In contrast, we observed a marked difference in subcutaneous adipocyte size when comparing HFD-fed $SMRT^{+/-}$ and WT mice. Whereas WT mice fed a HFD showed a marked increase in adipocyte size (mean area, 1488 ± 58.85 μm^2), diet-induced hypertrophy was much less pronounced in HFD-fed $SMRT^{+/-}$ mice (1042 ± 35.55 μm^2). In particular, subcutaneous WAT adipocytes from HFD-fed $SMRT^{+/-}$ mice were ~40% smaller than that of similarly fed WT mice (Fig. 2, *F* and *G*). These data indicate that SMRT deficiency results in expanded WAT, likely due to increased adipocyte number in response to HFD.

Previous studies have suggested that SMRT regulates adipogenesis, but these studies have not been performed in primary cells. For example, we previously showed that SMRT plays a crucial role in adipogenesis of 3T3-L1 cells (26). In addition, Nofsinger *et al.* (31) showed that knock-in of a $SMRT^{RID}$ mutation blocking interaction with NRs led to increased adipogenesis, but these studies were performed with transformed mouse embryonic fibroblast (MEF) cell lines. To assess the source of adipocyte hyperplasia seen in $SMRT^{+/-}$ mice, we compared the capacity of non-transformed primary MEFs with or without SMRT, to accumulate lipids in response to adipogenic stimuli. Because we isolated MEFs at E13.5 for our adipogenesis study, we were able to obtain $SMRT^{-/-}$ embryos in addition to WT and $SMRT^{+/-}$ ones. In response to adipogenic stimuli, MEFs lacking SMRT exhibited enhanced ability to form large, lipid-laden droplets characteristic of mature adipocytes when compared with WT MEFs, whereas $SMRT^{+/-}$ MEFs displayed an intermediate phenotype (Fig. 3*A*). We therefore studied the expression of adipocyte proteins after induction of adipogenesis (Fig. 3*B*). PPARγ, C/EBPα, perilipin, and adiponectin protein levels were all significantly increased in $SMRT^{+/-}$ and $SMRT^{-/-}$ MEFs relative to that of WT MEFs throughout adipogenesis. Again, the effect of SMRT on adipogenesis appears to occur in a gene dose-dependent manner; $SMRT^{+/-}$ MEFs differentiate better than WT MEFs, but less well than $SMRT^{-/-}$ MEFs.

$SMRT^{+/-}$ Mice Exhibit Decreased Adipocyte Leptin Expression on HFD, Leading to Increased Caloric Intake—Next, we assessed the expression of leptin and other adipocyte-specific proteins in mature epididymal WAT of HFD-fed mice by Western blotting. Interestingly, we found that leptin protein expression in $SMRT^{+/-}$ WAT was lower than in WT mice (Fig. 4*A*). PPARγ and perilipin expression were increased, as might be expected based on the previous adipogenesis data; surprisingly, we found no obvious difference in the expression of C/EBPα. To determine the cause of decreased adipocyte leptin protein expression, we performed quantitative RT-PCR analysis and found that leptin mRNA levels were correspondingly lower in $SMRT^{+/-}$ WAT (Fig. 4*B*). These data suggest that decreased leptin protein expression is most likely due to aberrant SMRT regulation of leptin gene expression, though an effect on leptin mRNA stability cannot be completely excluded.

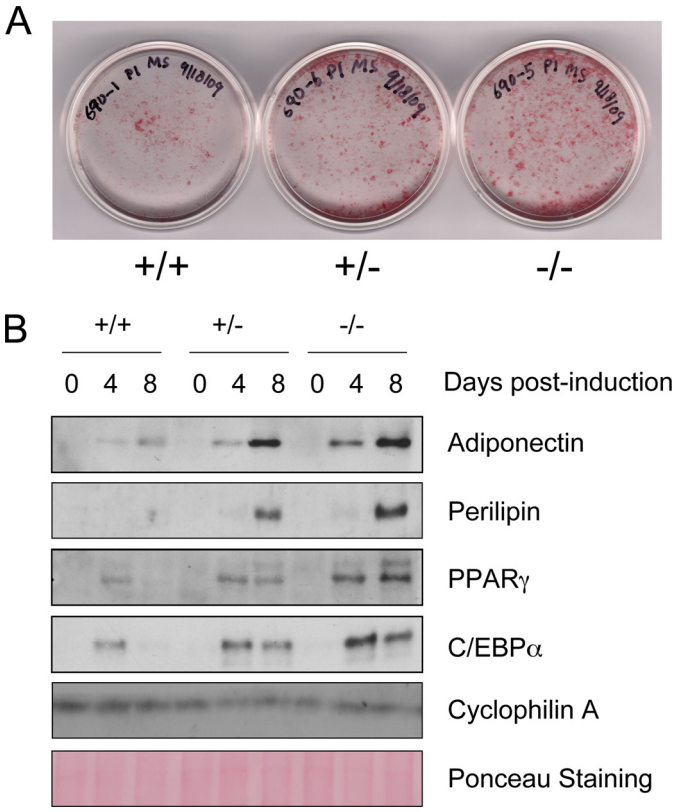

FIGURE 3. **Enhanced adipogenesis in the absence of SMRT.** *A*, Oil red O staining of WT, $SMRT^{+/-}$, and $SMRT^{-/-}$ MEFs that were induced to differentiate into adipocytes for 8 days. *B*, Western blot analysis of perilipin, adiponectin, PPARγ, and C/EBPα expression during differentiation of MEFs. Cells were harvested at the indicated times after the induction of adipogenesis.

To determine if decreased adipocyte leptin expression led to altered systemic leptin levels, we evaluated serum levels of leptin. On a chow diet, leptin levels were similar in WT and $SMRT^{+/-}$ mice (Fig. 4*C*). High-fat feeding led to an increase in leptin levels in both genotypes, but we observed significantly lower circulating leptin levels in HFD-fed $SMRT^{+/-}$ mouse sera when compared with WT controls (Fig. 4*C*). Thus, decreased adipocyte leptin expression leads to decreased circulating leptin levels in the setting of HFD. This is in contrast to most other models of diet-induced obesity, where circulating leptin levels usually reflect the degree of whole-body adiposity (10, 11). Instead, these data suggest that the reduced leptin levels seen in HFD-fed $SMRT^{+/-}$ mice might in fact lead to increased caloric intake. Therefore, we monitored food intake of $SMRT^{+/-}$ and WT mice. On a regular diet, at which time leptin levels were similar (Fig. 4*C*) there was no significant difference in food intake (data not shown), but on a HFD, $SMRT^{+/-}$ mice ate significantly more food (Fig. 4*D*). Thus, leptin is relatively decreased in the setting of high-fat feeding,

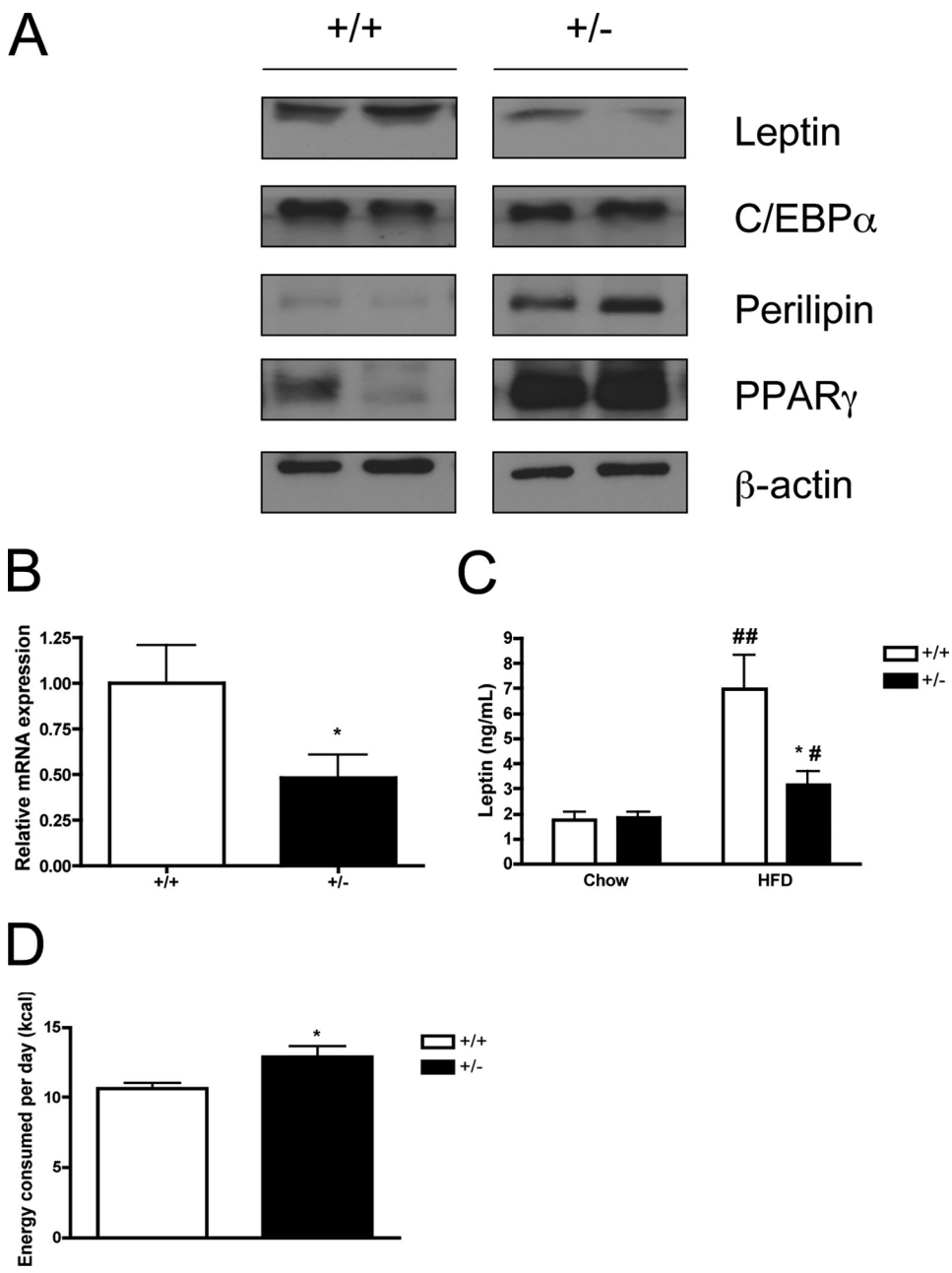

FIGURE 4. **Alterations in leptin expression in SMRT$^{+/-}$ mice fed a HFD.** *A*, Western blot analysis of leptin, C/EBPα, perilipin, and PPARγ expression in epididymal fat pads isolated from 3-month-old mice fed a HFD. *B*, real-time quantitative RT-PCR analysis of leptin mRNA in subcutaneous adipocytes of 3-month-old mice fed a HFD, $n = 8$. *C*, serum leptin levels in 3-month-old SMRT$^{+/-}$ and SMRT$^{+/+}$ mice fed either standard chow or HFD, $n = 7$–11. *D*, energy intake of 3-month-old SMRT$^{+/-}$ and WT mice fed a HFD, $n = 9$. *, $p < 0.05$ *versus* the corresponding WT value, while #, $p < 0.05$; ##, $p < 0.0005$ *versus* the corresponding chow value.

and decreased leptin levels lead to higher energy intake and adiposity.

To determine if the increased caloric intake was associated with alterations in energy usage, we measured locomotor activity, resting energy expenditure, oxygen consumption (VO_2) and carbon dioxide production (VCO_2) over a period of 3 days. There was no difference in locomotor activity between SMRT$^{+/-}$ and WT mice on HFD (Fig. 5*A*). Interestingly, we observed that heat production, which reflects total energy expenditure, was lower in SMRT$^{+/-}$ mice, particularly during the dark phase (Fig. 5*B*). However, this finding is unlikely to explain the increased adiposity specifically seen on HFD, since reduced heat production was also seen when the mice were fed a chow diet (data not shown). To evaluate whether this alteration in resting energy expenditure was associated with alterations in thyroid hormone levels, we measured TSH, T4, and T3 levels, but found that they were unchanged (Fig. 5*C*). In addition, core body temperature was also similar between the genotypes (Fig. 5*D*). Despite comparable respiratory exchange ratios (RERs) indicating similar preferences for the type of fuel substrate used (Fig. 5*E*), there was a balanced decrease in both of its components, VO_2 and VCO_2 in SMRT$^{+/-}$ mice (data not shown).

HFD-fed SMRT$^{+/-}$ Mice Have Reduced Hepatic Steatosis—Because SMRT$^{+/-}$ mice exhibit increased adiposity, we were interested in examining possible alterations in ectopic lipid accumulation. Therefore, we examined the lipid content in the frozen liver sections of HFD-fed by Oil Red O staining. We did not observe significant hepatic lipid accumulation in the livers of both SMRT$^{+/-}$ and SMRT$^{+/+}$ mice after 4 weeks of high-fat feeding (data not shown), which might have been due to the brevity of the feeding regimen. Therefore, we extended the duration of high-fat feeding to 8 weeks, which has been reported to be sufficient to induce hepatic steatosis in mice (36). After 8 weeks of HFD, we observed hepatic lipid accumulation in both SMRT$^{+/-}$ and WT mice (Fig. 6, *A* and *B*). However, we observed significantly reduced lipid storage in SMRT$^{+/-}$ liver compared with that of WT mice, indicating that despite the increased susceptibility of SMRT$^{+/-}$ mice to diet-induced obesity, they have reduced extra-adipose lipid deposition and/or formation. Interestingly, the reduction in hepatic lipid accumulation occurs despite similar circulating levels of free fatty acids (FFAs), glycerol and triglycerides in these animals (data not shown), likely due to the complex regulation of SMRT on the levels of these metabolites *in vivo*.

SMRT$^{+/-}$ Mice Are Protected from HFD-induced Insulin Resistance Due to Improved Adipocyte Insulin Sensitivity—We next investigated the role of SMRT in systemic and adipocyte insulin sensitivity. Interestingly, despite their increased

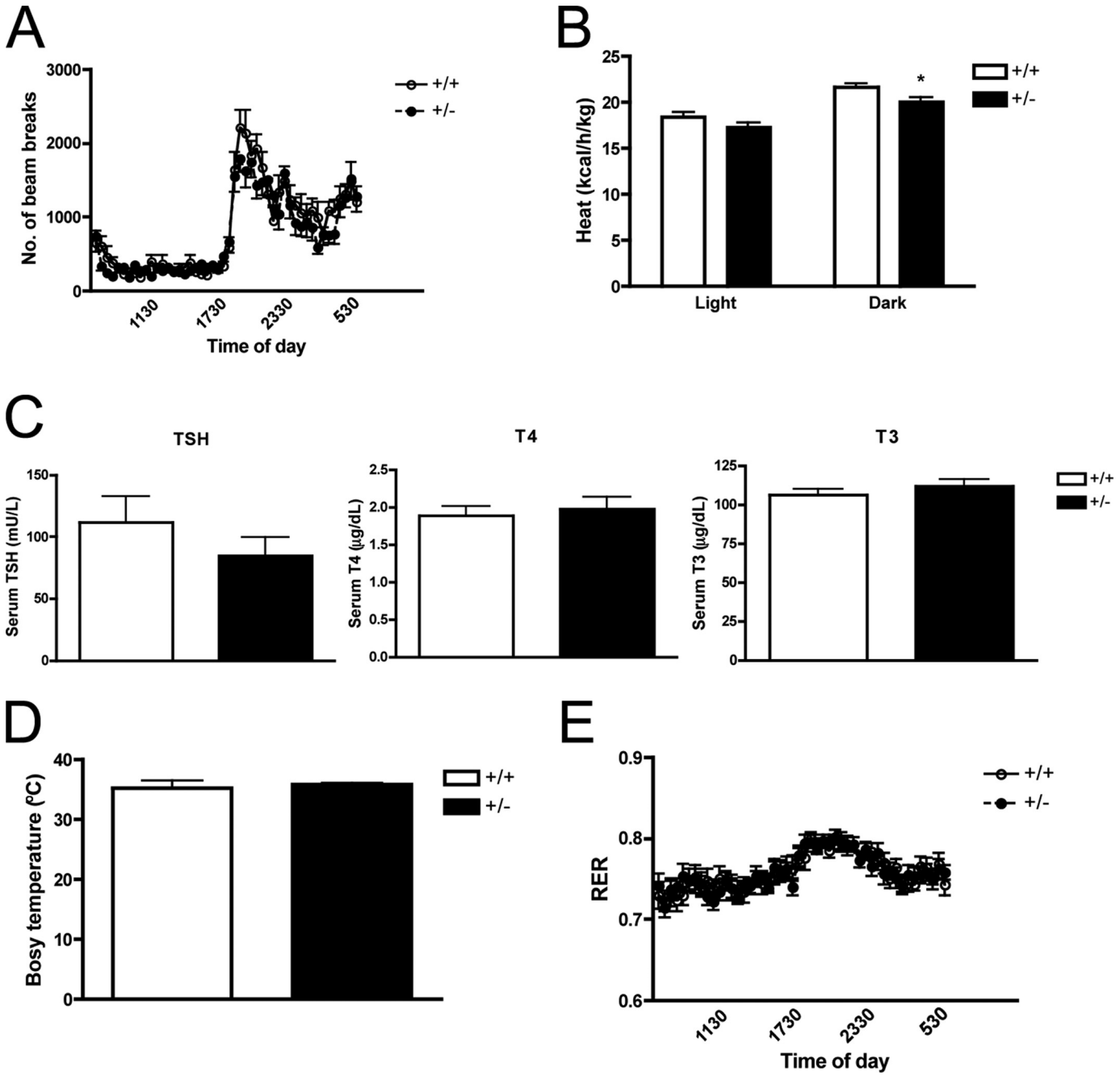

FIGURE 5. **Calorimetric parameters and thyroid function tests.** High-fat fed 3-month-old mice were placed in individual metabolic cages and acclimated to the chambers for 2–3 days before the 3-day measurement. *A* and *B*, locomotor activity (*A*) and heat production (*B*) was measured by indirect calorimetry, $n = 12$. *C*, serum TSH, T4 and T3 determined in high-fat fed 3-month-old mice, $n = 10–13$. *D*, core body temperature, measured using a mouse rectal probe, $n = 5–9$. *E*, respiratory exchange ratio determined by indirect calorimetry, as above, $n = 12$. *, $p < 0.05$ *versus* the corresponding WT value.

weight gain on HFD, glucose tolerance of $SMRT^{+/-}$ mice is comparable to that of HFD-fed WT mice (Fig. 6*C*). Although fasting insulin levels were similar at the start of the GTT, we found reduced insulin levels in response to a glucose bolus in $SMRT^{+/-}$ mice (Fig. 6*D*), suggesting decreased insulin requirements to maintain a similar level of glycemia. These data raise the possibility that $SMRT^{+/-}$ mice may be protected from the development of HFD-induced insulin resistance. Of note, Nofsinger *et al.* (31) showed that homozygous $SMRT^{mRID}$ mice had worse glucose tolerance than WT mice, but this was on a non-HFD regimen and appeared to be due to a muscle defect. We next performed insulin tolerance tests to examine insulin-mediated glucose disposal. As shown in Fig. 6*E*, the glucose-lowering effect of insulin was greater in $SMRT^{+/-}$ mice than it was in $SMRT^{+/+}$ mice on HFD. SMRT regulation of systemic insulin sensitivity is likely to be complex, and is dependent on SMRT effects in muscle and liver in addition to fat. In fact, SMRT actions in these various tissues may even have opposing effects. Our data, though, indicate that $SMRT^{+/-}$ mice are protected from developing insulin resistance on HFD, despite being more susceptible to diet-induced obesity.

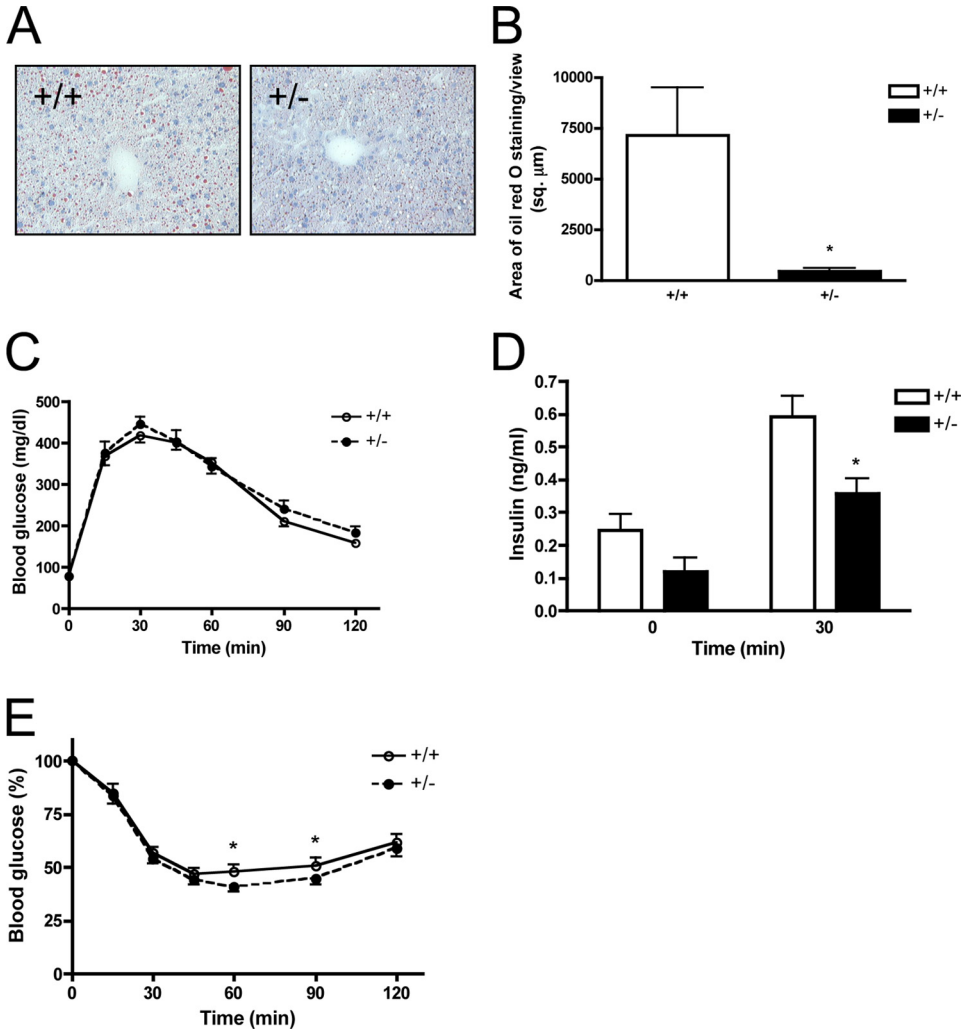

FIGURE 6. **HFD-fed SMRT$^{+/-}$ mice exhibit reduced hepatic steatosis and increased insulin-mediated glucose disposal.** *A*, oil red O staining of liver sections obtained from 4-month-old mice fed a HFD. *B*, quantification of liver oil red O staining from *A*, $n = 4$. *C* and *D*, glucose tolerance test. Blood glucose (*C*) and serum insulin (*D*) levels in 3-month-old SMRT$^{+/-}$ and WT mice fed a HFD were determined at the indicated times following intraperitoneal injection with a bolus of glucose, $n = 8–13$. *E*, insulin tolerance test. Blood glucose levels in 3-month-old SMRT$^{+/-}$ and WT mice fed a HFD were determined at the indicated times following intraperitoneal injection with a bolus of insulin, $n = 21–26$. *, $p < 0.05$ *versus* the corresponding WT value.

To specifically assess the contribution of SMRT in regulating adipocyte insulin sensitivity, we examined the ability of insulin to induce Akt phosphorylation in freshly isolated primary adipocytes *ex vivo*. We treated primary adipocytes from both SMRT$^{+/-}$ and WT mice with or without insulin (1, 10, or 100 nM) for 15 min. The lysates were then analyzed by SDS-PAGE for phosphorylated and total Akt protein levels. As shown in Fig. 7*A*, Akt phosphorylation in response to insulin treatment is more robust in SMRT$^{+/-}$ primary adipocytes isolated from both epididymal and subcutaneous WATs (Fig. 7*A*). We quantified the extent of insulin-stimulated Akt phosphorylation in primary adipocytes by densitometry and found that SMRT$^{+/-}$ adipocytes have significantly increased Akt phosphorylation in response to insulin treatment (Fig. 7*B*). Thus, enhanced insulin signaling in WAT of SMRT$^{+/-}$ mice may partially account for the protection from HFD-induced insulin resistance observed in SMRT$^{+/-}$ mice.

To further evaluate the adipocyte contribution to the systemic insulin sensitivity in SMRT$^{+/-}$ mice, we conducted lipolysis assays using freshly isolated primary adipocytes. We treated the primary adipocytes with or without 10 μM isoproterenol and/or 1 nM insulin. We assessed lipolysis by measuring the amount of glycerol released into the media and found that rates of basal and isoproterenol-induced lipolysis are similar in SMRT$^{+/-}$ and WT adipocytes (Fig. 7*C*). However, the ability of insulin to suppress lipolysis, as measured by glycerol release, is enhanced in SMRT$^{+/-}$ adipocytes (Fig. 7*D*). These data confirm that SMRT$^{+/-}$ adipocytes are more insulin sensitive than WT adipocytes when the mice are fed a HFD. Interestingly, isoproterenol-induced and insulin-suppression of FFA release were markedly increased in subcutaneous SMRT$^{+/-}$ adipocytes, while they were not significantly altered in epididymal adipocytes (Fig. 7, *E* and *F*). The differences in the FFA and glycerol results between the two depots may be due to the complex role that SMRT plays in regulating adipocyte function.

DISCUSSION

Obesity is a rapidly escalating phenomenon that constitutes a major threat to human health internationally. An alarming increase in the incidence of obesity and the unprecedented presentation of type 2 diabetes in the pediatric population is increasing the urgency of this issue (37, 38). Although drastic therapeutic interventions are needed, effective therapeutic options are limited and preventive measures have had limited success. As an active and indispensable endocrine organ involved in the regulation of energy homeostasis, the adipose tissue plays a fundamental role in the pathogenesis of obesity-related pathologies (1, 2). Thus, it is vital to elucidate the molecular mechanism of adipocyte differentiation and understand factors that affect adipocyte function.

We have previously shown that SMRT ablation resulted in enhanced adipocyte differentiation of 3T3-L1 preadipocytes, in part through increased PPARγ transcriptional activity (26). Activation of Sirt1, which forms a complex with PPARγ and SMRT, also decreases fat accumulation in mature adipocytes (39). Nofsinger *et al.*, showed that SMRT is an integrator of glucose metabolism and whole body metabolic homeostasis (31), but its specific role in the adipocyte is unclear. In this

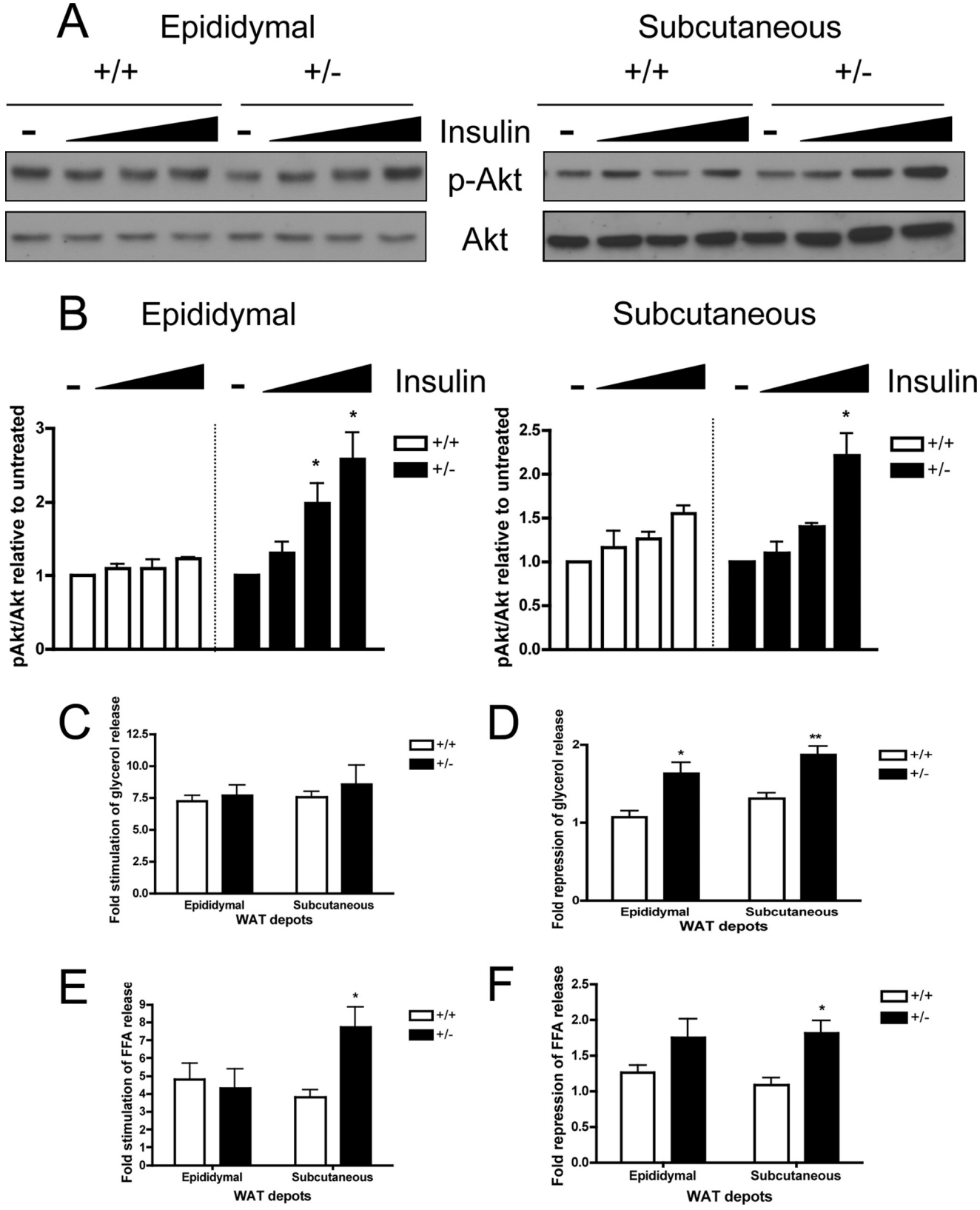

FIGURE 7. **Increased WAT insulin sensitivity in SMRT$^{+/-}$ mice fed a HFD.** *A*, primary adipocyte insulin signaling. Western blot analysis of Ser-473-phosphorylated Akt (p-Akt) and total Akt in primary adipocytes isolated from the epididymal WAT (*left*) and subcutaneous WAT (*right*) in response to insulin treatment. *B*, ImageJ quantification of Akt phosphorylation with insulin treatment in primary adipocytes from *A*, $n = 4–5$. *C–F*, primary adipocyte lipolysis assay. Rate of lipolysis in freshly isolated primary adipocytes isolated from SMRT$^{+/-}$ and WT mice fed a HFD was determined by measuring glycerol content (*C* and *D*) and free fatty acid content (*E* and *F*) in the medium, with or without isoproterenol or insulin treatment. Fold-stimulation and fold-repression of lipolysis by isoproterenol and insulin respectively were calculated, $n = 5–7$. *, $p < 0.05$; **, $p < 0.01$ *versus* the corresponding WT value.

study, we investigated the effect of SMRT on adipogenesis, leptin expression, and adipocyte insulin sensitivity. Our results demonstrate that SMRT plays a crucial role in regulating adipocyte function *in vivo*.

Because of the embryonic lethality of homozygous SMRT knock-out ($SMRT^{-/-}$) mice (29, 30), we studied heterozygous SMRT ($SMRT^{+/-}$) knock-out mice and their wild-type (WT) littermates. We found that $SMRT^{+/-}$ mice exhibit increased adiposity when they are placed on a HFD. $SMRT^{+/-}$ mice gained more weight on HFD diet, and the weight gain is specifically attributable to the expansion in WAT. We showed that this phenotype seen is attributable to a combination of both increased adipocyte hyperplasia, decreased adipocyte leptin expression, and increased food intake. Moreover, our data indicated that MEFs derived from SMRT-deficient embryos exhibit greater adipogenesis, suggesting that the adipocyte hyperplasia seen in $SMRT^{+/-}$ mice may be due in part to enhanced adipogenesis *in vivo* as well. Previous work demonstrated the importance of SMRT in adipocyte differentiation *in vitro* (26, 31), but this is the first report utilizing primary, nontransformed MEFs to define the role of SMRT in adipogenesis. Interestingly, the increase in adipocyte hyperplasia in SQ WAT is associated with a greater percentage of relatively smaller adipocytes, which have been associated with improved metabolic function (40).

Intriguingly, $SMRT^{+/-}$ mice exhibit significantly reduced leptin levels despite their obese phenotype when placed on HFD. This runs counter to many other models of diet-induced obesity. $SMRT^{+/-}$ mice on HFD had decreased serum leptin levels, and primary adipocytes from these mice exhibited decreased leptin mRNA and protein expression. The regulation of leptin gene expression by PPARγ remains controversial. However, multiple studies report that TZD treatment reduces leptin levels in 3T3-L1 adipocytes (41), rodents (42) and humans (43). Therefore, it is possible that enhanced PPARγ signaling in the setting of decreased SMRT leads to a decline in leptin expression. However, it should be noted that negative regulation by PPARγ is complex, and the role of SMRT on leptin expression, whether direct or indirect, remains unclear. Future experiments will define the underlying mechanisms for these findings.

Nofsinger *et al.* (31) also identified a role for SMRT in metabolic tissues *in vivo* using a $SMRT^{mRID}$ model, but our findings differ in a number of respects. First, our model is a knock-out of SMRT that reduces SMRT protein levels while the $SMRT^{mRID}$ model is a knock-in mutation that renders SMRT unable to interact with NRs. Therefore certain differences in phenotype may depend on non-NR transcription factor interactions with SMRT. In addition, the $SMRT^{mRID}$ phenotype was studied in homozygous mice on chow diet; in contrast, our study utilized heterozygous mice and the phenotype was induced by high-fat feeding. Whereas $SMRT^{mRID}$ mice have decreased body weight, our $SMRT^{+/-}$ mice exhibit increased body weight on HFD due to expansion of SQ and visceral WAT depots. Strikingly, despite significantly increased WAT in response to high-fat feeding, adipocytes derived from $SMRT^{+/-}$ mice are more insulin-sensitive than WT adipocytes. Importantly, both studies used generalized models, and tissue-specific models of SMRT deficiency will have to be generated to more fully define the role of SMRT in distinct metabolic tissues.

Interestingly, the metabolic phenotype seen in $SMRT^{+/-}$ mice mirrors clinical observations of type 2 diabetic patients treated with TZDs. For example, TZDs are known to improve insulin sensitivity, yet are associated with increased fat mass (17, 18). Our work (26) and other (44, 31) suggests that SMRT regulates PPARγ action, and $SMRT^{mRID}$ mice show significant alterations in PPARγ-regulated genes (31). Thus, it is likely that alterations in PPARγ action underlie many of the changes seen in our mice. Because selective PPARγ modulators (SPPARMs) are in development to improve TZD efficacy while reducing side effects (45), it will be necessary to take into consideration the role of SMRT in PPARγ biology.

In summary, this study highlights the important role that SMRT plays in energy homeostasis and adipocyte function *in vivo*. In the setting of decreased SMRT levels, mice exhibit increased adiposity and susceptibility to diet-induced obesity. Surprisingly, however, this increased adiposity is associated with improved adipocyte insulin sensitivity. These findings lend support to the hypothesis that an impairment in the ability to expand fat mass appropriately in the setting of positive energy balance leads to metabolic derangements such as Type 2 diabetes (40). SMRT deficiency results in the expansion of fat mass, but particularly in the formation of smaller, more insulin-sensitive adipocytes rather than adipocyte hypertrophy. By increasing the number of smaller adipocytes, adipocyte insulin sensitivity is maintained even in the setting of high-fat feeding. In addition, our data supports the idea that hyperleptinemia during diet-induced obesity results from adipocyte hypertrophy rather than hyperplasia. In $SMRT^{+/-}$ mice, an increase in adiposity caused by increased adipocyte number is associated with a relative decrease in leptin levels. Further studies will further define the underlying mechanisms by which SMRT regulates insulin sensitivity in the setting of increased adiposity.

Acknowledgments—We thank Xiaohui Liao for performing the thyroid function studies and Graeme Bell, Roy Weiss, Skip Garcia, and Jun Liu for helpful discussions. We would also like to thank the University of Chicago Diabetes Research and Training Center (supported by National Institutes of Health Grant P60 DK20595) for use of metabolic cages.

REFERENCES

1. Flier, J. S. (2004) *Cell* **116,** 337–350
2. Spiegelman, B. M., and Flier, J. S. (2001) *Cell* **104,** 531–543
3. Zhang, Y., Proenca, R., Maffei, M., Barone, M., Leopold, L., and Friedman, J. M. (1994) *Nature* **372,** 425–432
4. Cowley, M. A., Smart, J. L., Rubinstein, M., Cerdán, M. G., Diano, S., Horvath, T. L., Cone, R. D., and Low, M. J. (2001) *Nature* **411,** 480–484
5. Schwartz, M. W., Seeley, R. J., Campfield, L. A., Burn, P., and Baskin, D. G. (1996) *J. Clin. Invest.* **98,** 1101–1106
6. Schwartz, M. W., Seeley, R. J., Woods, S. C., Weigle, D. S., Campfield, L. A., Burn, P., and Baskin, D. G. (1997) *Diabetes* **46,** 2119–2123
7. Frühbeck, G., Aguado, M., and Martínez, J. A. (1997) *Biochem. Biophys. Res. Commun.* **240,** 590–594
8. Muoio, D. M., Dohm, G. L., Fiedorek, F. T. Jr., Tapscott, E. B., and Coleman, R. A. (1997) *Diabetes* **46,** 1360–1363
9. Zhou, Y. T., Shimabukuro, M., Koyama, K., Lee, Y., Wang, M. Y., Trieu, F.,

Newgard, C. B., and Unger, R. H. (1997) *Proc. Natl. Acad. Sci. U.S.A.* **94,** 6386–6390
10. Ahrén, B., Månsson, S., Gingerich, R. L., and Havel, P. J. (1997) *Am. J. Physiol.* **273,** R113–R120
11. Maffei, M., Halaas, J., Ravussin, E., Pratley, R. E., Lee, G. H., Zhang, Y., Fei, H., Kim, S., Lallone, R., and Ranganathan, S. (1995) *Nat. Med.* **1,** 1155–1161
12. Kolaczynski, J. W., Considine, R. V., Ohannesian, J., Marco, C., Opentanova, I., Nyce, M. R., Myint, M., and Caro, J. F. (1996) *Diabetes* **45,** 1511–1515
13. Trayhurn, P., Thomas, M. E., Duncan, J. S., and Rayner, D. V. (1995) *FEBS Lett.* **368,** 488–490
14. Rosen, E. D., Sarraf, P., Troy, A. E., Bradwin, G., Moore, K., Milstone, D. S., Spiegelman, B. M., and Mortensen, R. M. (1999) *Mol. Cell* **4,** 611–617
15. Tamori, Y., Masugi, J., Nishino, N., and Kasuga, M. (2002) *Diabetes* **51,** 2045–2055
16. Lehmann, J. M., Moore, L. B., Smith-Oliver, T. A., Wilkison, W. O., Willson, T. M., and Kliewer, S. A. (1995) *J. Biol. Chem.* **270,** 12953–12956
17. Kelly, I. E., Han, T. S., Walsh, K., and Lean, M. E. (1999) *Diabetes Care* **22,** 288–293
18. Mori, Y., Murakawa, Y., Okada, K., Horikoshi, H., Yokoyama, J., Takima, N., and Ikeda, Y. (1999) *Diabetes Care* **22,** 908–912
19. Adams, M., Montague, C. T., Prins, J. B., Holder, J. C., Smith, S. A., Sanders, L., Digby, J. E., Sewter, C. P., Lazar, M. A., Chatterjee, V. K., and O'Rahilly, S. (1997) *J. Clin. Invest.* **100,** 3149–3153
20. Sewter, C. P., Blows, F., Vidal-Puig, A., and O'Rahilly, S. (2002) *Diabetes* **51,** 718–723
21. Lonard, D. M., and O'Malley, B. W. (2005) *Trends Biochem. Sci.* **30,** 126–132
22. Feige, J. N., and Auwerx, J. (2007) *Trends Cell Biol.* **17,** 292–301
23. Chen, J. D., and Evans, R. M. (1995) *Nature* **377,** 454–457
24. Hörlein, A., Näär, A. M., Heinzel, T., Torchia, J., Gloss, B., Kurokawa, R., Ryan, A., Kamei, Y., Söderström, M., and Glass, C. K. (1995) *Nature* **377,** 397–404
25. Sande, A., and Privalsky, M. L. (1996) *Mol. Endocrinol.* **10,** 813–825
26. Yu, C., Markan, K., Temple, K. A., Deplewski, D., Brady, M. J., and Cohen, R. N. (2005) *J. Biol. Chem.* **280,** 13600–13605
27. Ghisletti, S., Huang, W., Jepsen, K., Benner, C., Hardiman, G., Rosenfeld, M. G., and Glass, C. K. (2009) *Genes Dev.* **23,** 681–693
28. Yu, J., Palmer, C., Alenghat, T., Li, Y., Kao, G., and Lazar, M. A. (2006) *Cancer Res.* **66,** 9316–9322
29. Jepsen, K., Solum, D., Zhou, T., McEvilly, R. J., Kim, H. J., Glass, C. K., Hermanson, O., and Rosenfeld, M. G. (2007) *Nature* **450,** 415–419
30. Jepsen, K., Gleiberman, A. S., Shi, C., Simon, D. I., and Rosenfeld, M. G. (2008) *Genes Dev.* **22,** 740–745
31. Nofsinger, R. R., Li, P., Hong, S. H., Jonker, J. W., Barish, G. D., Ying, H., Cheng, S. Y., LeBlanc, M., Xu, W., Pei, L., Pei, L., Kang, Y. J., Nelson, M., Downes, M., Yu, R. T., Olefsky, J. M., Lee, C. H., and Evans, R. M. (2008) *Proc. Natl. Acad. Sci. U.S.A.* **105,** 20021–20026
32. Wabitsch, M., Brenner, R. E., Melzner, I., Braun, M., Möller, P., Heinze, E., Debatin, K. M., and Hauner, H. (2001) *Int. J. Obes. Relat. Metab. Disord.* **25,** 8–15
33. Jurczak, M. J., Danos, A. M., Rehrmann, V. R., Allison, M. B., Greenberg, C. C., and Brady, M. J. (2007) *Am. J. Physiol. Endocrinol. Metab.* **292,** E952–E963
34. Di Cosmo, C., Liao, X. H., Dumitrescu, A. M., Weiss, R. E., and Refetoff, S. (2009) *Endocrinology* **150,** 4450–4458
35. Pohlenz, J., Schönberger, W., Koffler, T., and Refetoff, S. (1999) *Thyroid* **9,** 1001–1004
36. Gauthier, M. S., Couturier, K., Charbonneau, A., and Lavoie, J. M. (2004) *Int. J. Obes. Relat. Metab. Disord.* **28,** 1064–1071
37. Narayan, K. M., Boyle, J. P., Thompson, T. J., Sorensen, S. W., and Williamson, D. F. (2003) *JAMA* **290,** 1884–1890
38. Rocchini, A. P. (2002) *N. Engl. J. Med.* **346,** 854–855
39. Picard, F., Kurtev, M., Chung, N., Topark-Ngarm, A., Senawong, T., Machado De Oliviera, R., Reid, M., McBurney, M. W., and Guarente, L. (2004) *Nature* **429,** 771–776
40. Kim, J. Y., van de Wall, E., Laplante, M., Azzara, A., Trujillo, M. E., Hofmann, S. M., Schraw, T., Durand, J. L., Li, H., Li, G., Jelicks, L. A., Mehler, M. F., Hui, D. Y., Deshaies, Y., Shulman, G. I., Schwartz, G. J., and Scherer, P. E. (2007) *J. Clin. Invest.* **117,** 2621–2637
41. Kallen, C. B., and Lazar, M. A. (1996) *Proc. Natl. Acad. Sci. U.S.A.* **93,** 5793–5796
42. De Vos, P., Lefebvre, A. M., Miller, S. G., Guerro-Millo, M., Wong, K., Saladin, R., Hamann, L. G., Staels, B., Briggs, M. R., and Auwerx, J. (1996) *J. Clin. Invest.* **98,** 1004–1009
43. Shimizu, H., Tsuchiya, T., Sato, N., Shimomura, Y., Kobayashi, I., and Mori, M. (1998) *Diabetes Care* **21,** 1470–1474
44. Guan, H. P., Ishizuka, T., Chui, P. C., Lehrke, M., and Lazar, M. A. (2005) *Genes Dev.* **19,** 453–461
45. Balint, B. L., and Nagy, L. (2006) *Endocr. Metab. Immune. Disord. Drug Targets* **6,** 33–43